Buckling resistance of hot-finished CHS beam-columns using FE modeling and machine learning

Musab Rabi [1*], Ikram Abarkan [2], Rabee Shamass [3]

[1] Dept of Civil Engineering, Jerash University, Jordan

[2] Department of Physics, Faculty of Sciences, Abdelmalek Essaâdi University, 93002 Tetouan, Morocco

[3] Division of Civil and Building Services Engineering, School of Build Environment and Architecture, London South Bank University, UK

Abstract

The use of circular hollow sections (CHS) has increased in recent years owing to its excellent mechanical behaviour including axial compression and torsional resistance as well as its aesthetic appearance. They are popular in a wide range of structural members including beams, columns, trusses and arches. The behaviour of hot-finished CHS beam-columns made from normal and high strength steel is the main focus of this paper. A particular attention is given to predict the ultimate buckling resistance of CHS beam-columns using the recent advancement of the artificial neural network (ANN). FE models were established and validated to generate an extensive parametric study. The ANN model is trained and validated using a total of 3439 data points collected from the generated FE models and experimental tests available in the literature. A comprehensive comparative analysis with the design rules in Eurocode 3 is conducted to evaluate the performance of the developed ANN model. It is shown that the proposed ANN based design formula provides a reliable means for predicting the buckling resistance of the CHS beam-columns. This formula can be easily implemented in any programming software, providing an excellent basis for engineers and designers to predict the buckling resistance resistance of the CHS beam-columns with a straightforward procedure in an efficient and sustainable manner with least computational time

Keywords: Artificial neural networks (ANN), Eurocode 3, FE modelling, Hot-finished CHS beam-columns, Normal and high strength steels.

1 Introduction

Circular hollow sections (CHS) are being increasingly used in a wide range of structural members including beams, columns, trusses, arches and wind turbine towers. They are popular owing to its outstanding performance in compression, excellent torsional resistance and aesthetic appearance. CHS members with high strength steel have gain more recognition and attention by structural designers and practicing engineers owing to the exceptional benefits from high strength steels and hollow sections. The typically definition for high strength steels are those with steel grades of S460 or above [1]. High strength CHS members offer high strength-to-weight ratio, lighter cross-sectional area, long-span structures and reduced carbon footprint. They are used for heavily loaded members, particularly where the steel members would otherwise be very thick. Although high strength steels are more expensive than the normal strength steels, they are often seen as more efficient and economic material given the reductions in the material usage and other cost savings associated with fabrication, handling and transportation [2], [3].

The design rules for CHS beam-columns are specified in the latest version of EC3 – prEN 1993-1-1:2020 [4]. Both high strength and normal strength CHS are readily available as cold-formed and hot- finished products as given in EN 10210-2:2019 [5] and EN 10219-2:2019 [6], respectively, as well as fabricated CHS products (typically produced by forming and welding a steel sheet into a circular shape). There is a general scarcity of experimental research on the structural behaviour and design of CHS beam-columns including hot-finished [7-10], cold finished [8, 11-13] and fabricated CHS [14-15]. The cold-formed CHS exhibit a continuous rounded stress–strain response caused by cold-working throughout the forming process, whereas the hot-finished CHS have a linear elastic response followed by well-defined yield plateau and moderate degree of strain hardening [16-21]. More recently, Meng and Gardner [22] conducted a series of experimental and numerical tests on hot-finished and cold-formed CHS beam-columns made from both normal and high strength steels. Further experimental and numerical research work on CHS beam-columns is still considered necessary for providing accurate assessment and improvement of current design standards. In this paper, a particular attention is given to the hot-finished CHS beam-columns made of normal and high strength steels.

The rapid development of advanced computerised systems has been shown to be an efficient and reliable means for predicting the structural behaviour of steel members. In this context, Artificial Neural Network (ANN) presents one of the most well-known techniques of artificial intelligence which is used to solve complex nonlinear problems providing an accurate prediction of the structural performance of members [23- 24]. ANN typically consists of the input layer and output layer which are interconnected using intermediate hidden layer. The hidden layer is comprised of several weighted connections between the input and output parameters known as neurons. The quality of the predicted output results principally depends on the number of neuron and the quality and quantity of the input data used to train the ANN.

The use of ANN has been becoming increasingly popular in predicting various structural behaviour in constructional steel elements including composite columns [25-27], beams [28-31], steel connections [32-34], frames [35], steel plates [36-38], cellular and castellated steel beam [39-44], cold-formed CHS beam-columns [45] and stainless steel reinforcement [46]. However, there is currently no available ANN research (at least in the available domain) on hot-finished CHS beam-columns. Therefore, this paper aims to study the buckling resistance of hot-finished CHS beam-columns made from both normal high strength steels by utilising the power of ANN. Detailed description on the development and validation of the ANN model is discussed. The ANN model is developed using a total of 3439 data points, obtained from a previously developed and validated numerical model performed by Meng and Gardner [22], and a limited number of experimental data available in [7-10]. Consequently, an ANN-based formula is proposed for predicting the buckling resistance capacity of hot-finished CHS beam-columns. In addition, an assessment of the current design rules given in the latest version of Eurocode 3 prEN 1993-1-1:2020 [4] for CHS beam-column is presented through a comparative analysis with ANN predictions and results from numerical and experimental data.

2 Eurocode 3 design rules

This section examines the stability design provisions provided in prEN 1993-1-1:2020 [4] for CHS beam-columns structural steel, with a particular focus given to the cross-section classifications and the beam-column interaction relationship. Cross-sections are categorised into four main groups based on the deformation capacity and the sensitivity to local buckling under a specified loading condition. For class 1 and 2, members can reach the full plastic cross-sectional resistance. However, class 1 cross-sections demonstrate a sufficient rotational capacity allowing for plastic design. For class 3, members are capable of only reaching the elastic cross-sectional resistance and do not achieve the plastic cross-sectional resistance owing to inelastic local buckling failure. Class 4 cross-sections are characterized by local buckling failure prior to reaching their elastic cross-sectional resistance. For each class, a specified slenderness limit is given in Eurocode 3 [4] in terms of $D/t\varepsilon^2$, where D is the outer diameter, t is the thickness and ε is a parameter equals to $(235/f_y)^{0.5}$, in which f_y denotes for the yield stress. These limits for CHS are set to be 50 and 70 for class 1 and 2, respectively. For class 3, A higher transition limit between 90 and 140 is adopted for the case of combined compression plus bending, in which the limit of 90 is taken for cross-sections with compression loading while 140 is taken for pure bending loading scenario. The transition limit is equal to 2520/(5ψ+23), where ψ is the ratio between the maximum and minimum cross-sectional stresses.

The beam-column interaction relationship specified in Eurocode 3 [4] can be simplified to Eq. 1, owing the axisymmetric geometry of CHS.

$$\frac{N_{ED}}{\chi N_{c,R}/\gamma_{M1}} + k\frac{M_{ED}}{M_{c,R}/\gamma_{M1}} \leq 1.0 \qquad (1)$$

In this expression, N_{Ed} and M_{Ed} represent the applied axial force and bending moment, respectively. k is the interaction factor, χ is the column buckling reduction factor and γ_{M1} is the partial safety factor taken as 1.0 for carbon steel members.

The cross-sectional resistances to compression ($N_{c,R}$) and bending ($M_{c,R}$) are determined as follows:

$$N_{c,R} = Af_y \qquad \text{for class 1-3 cross-sections} \qquad (2)$$

$$M_{c,R} = W_{pl}f_y \qquad \text{for class 1-2 cross-sections} \qquad (3)$$

$$M_{c,R} = W_{el}f_y \qquad \text{for class 3 cross-sections} \qquad (4)$$

where W_{el} and W_{pl} are the elastic and plastic section modulus. The column buckling reduction factor (χ) is calculated as shown in Eq. 5.

$$\chi = \frac{1}{\phi + \sqrt{\phi^2 + \lambda^2}} \leq 1 \qquad (5)$$

$$\lambda = \frac{N_{c,R}}{N_{cr}} \qquad \text{for class 1-3 cross-sections} \qquad (6)$$

$$\phi = 0.5(1 + \alpha(\lambda - 0.2) + \lambda^2) \qquad (7)$$

In which, N_{cr} is the Euler buckling load and λ is the relative slenderness. The codified values of the imperfection factor (α) are given in Table 1.

The interaction factor (k) is calculated using Eq. 8 for class 1-3 cross-sections, where C_m is a parameter accounting for the shape of the first-order bending moment diagram and is taken as unity (for constant bending moment). For class 4 cross-sections, the interaction factor is obtained on the basis of the effective cross-sectional area using different formula, which is out of the scope of this study.

$$k = C_m\left(1 + (\lambda - 0.2)\frac{N_{ED}}{\chi N_{c,R}/\gamma_{M1}}\right) \quad \text{for } \lambda \leq 1$$
$$k = C_m\left(1 + 0.8\frac{N_{ED}}{\chi N_{c,R}/\gamma_{M1}}\right) \quad \text{for } \lambda > 1 \qquad (8)$$

Table 1: Values for EC3 imperfection factor (α) for hollow sections.

Production method	α for steel strength (S235-S420)	α for steel strength (S460-S700)
Hot-finished	0.21	0.13
Cold-formed	0.49	0.49

3. Finite element modelling and validation

Finite element (FE) models were established using the general purpose FE software Abaqus [47] in order to examine the structural behaviour CHS beam-columns. The main aim is to conduct extensive parametric study using a validated FE model that can be used to train and validate the ANN model. A Similar approach to that in [22] and [48] was employed in to examine the buckling resistance capacity of hot-finished CHS beam-columns. The model was shown to accurately predict the behaviour in terms of load-deflection curve, ultimate bearing capacity and global and local buckling failure mode [22, 48].

3.1. Development of the FE model

The FE model was developed using Geometrically and materially nonlinear analyses with imperfections using the static Riks solver available in Abaqus software [47]. A typical FE model for CHS beam-column is presented in Fig. 1. A four-noded shell element with reduced integration (i.e. S4R) was employed, owing to its suitability for modelling thin walled structural elements [13, 49]. A fine mesh with an element size of $0.1\sqrt{Dt}$ was selected and found to accurately capture the general buckling behaviour. A reference point was created at the end sections in which all degrees of freedom were coupled. A pinned end boundary condition was applied to the reference point to simulate the knife edge steel plate used in the laboratory. Elastic buckling modes were introduced in the FE model to represent the local and global geometric imperfections. In addition, Residual stresses that is principally induced from uneven cooling were not explicitly considered in the modelling hot-finished CHS as it was shown to be relatively negligible for tubular sections with reference to the yield stress [50]. The material properties of the tested profiles were tested by means of tensile coupon test and reported by Meng and Gardner [48]. To reduce the computational time and cost, only a quarter-models of the CHS is designed assuming symmetrical boundary conditions along the length and the mid cross-sectional plane. Further detailed descriptions on the development of the FE model are given in more details in [48].

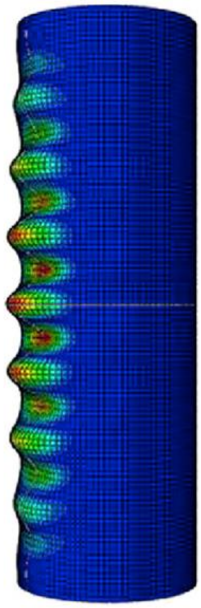

Fig. 1: Typical FE model for CHS beam-column [22].

3.2. Validation of the FE model

Fig. 2 illustrates comparison between the numerical and experimental load-mid height lateral deflection curves for one of the specimens. It is observed that the FE model demonstrates excellent depiction of the experimental response in terms of the initial stiffness, ultimate buckling resistance and failure mode. A comparison of the failure modes obtained experimentally and numerically are shown in Fig. 3. In order to provide a robust validation of the FE model, a comparison between the ultimate loads obtained numerically ($N_{u,FE}$) and experimentally ($N_{u,test}$) was conducted using four different global geometric imperfection amplitudes (ω_g) were employed, as presented in Table 2. The statistical results demonstrates that the buckling resistance of the CHS beam-columns is slightly influenced by the global geometric imperfection amplitudes (ω_g) and therefore a geometric imperfection value of the critical length (L_{cr})/1000 was selected to conduct the parametric study giving an accurate prediction with less computational time [22]. Accordingly, it was concluded that the developed FE model is capable of providing excellent and accurate resistance predictions of the hot-formed CHS beam-columns.

Table 2. Comparisons of buckling resistances obtained numerically and experimentally [22].

	$N_{u,FE}/N_{u,test}$

	Measured ω_g	$\omega_g = L_{cr}/2000$	$\omega_g = L_{cr}/1000$	$\omega_g = L_{cr}/500$
Mean	0.982	0.980	0.970	0.956
Coefficient of variation	0.027	0.026	0.030	0.034

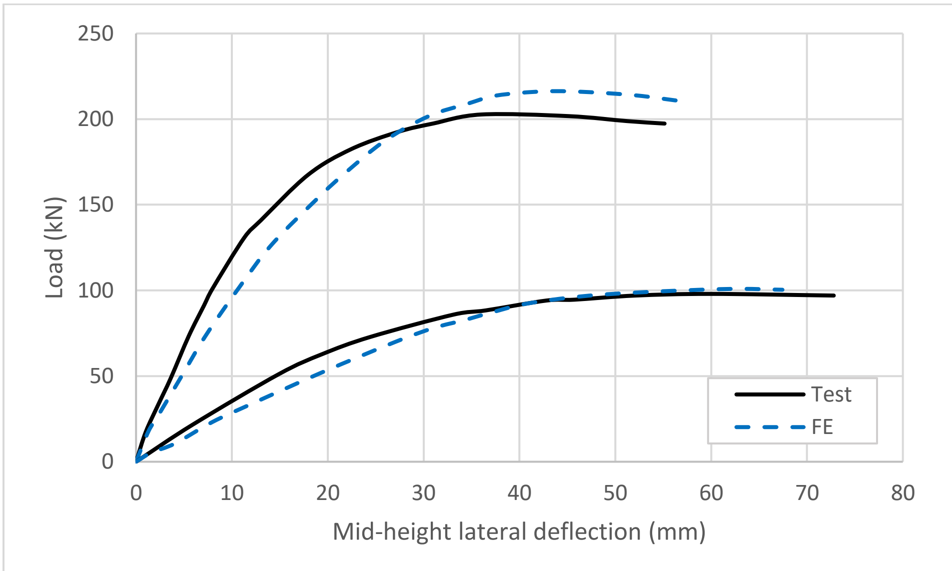

Fig. 2: Typical numerical and experimental load-deflection curves for hot-finished CHS beam-columns [22].

Fig. 3: Typical failure modes obtained experimentally and numerically [22].

3.3. Parametric study

A total of 3428 numerical models were conducted to expand the data pool and provide more predictions of the buckling resistance of CHS beam-columns. The parametric study covered a wide range of normal and high strength steels ranging from grade S355 to grade S900, as presented in Table 3 and given in EC3 [4]. Given that EC3 does not cover high strength steel grade S900, the yield and ultimate stress were assumed to be 900MPa and 945 MPa, respectively. The nominal value of elastic modulus E was assumed to be 210 000 MPa. Besides, the outer diameter of the CHS was fixed to 100 mm, but their thickness varied between 1.18 and 15 mm to accommodate a wide range of $D/t\varepsilon^2$ values up to the EC3 Class 3 limit, as described in section 2. The members' length was varied between 300 and 5300 mm, allowing for a wide variety of relative slenderness values λ (i.e. within 0.2-2). The initial eccentricities, which were equal at both end sides of the specimens, ranged between 2.4–360 mm to generate various loading combinations.

Table 3: Nominal mechanical properties for hot-finished and cold-formed hollow sections for Steel grade S355-900 [22].

Grade	E (MPa)	f_y (MPa)	f_u (MPa)
S355	210 000	355	490
S460	210 000	460	540
S550	210 000	550	600
S690	210 000	690	770
S900	210 000	900	945

4. Development of the artificial neural network (ANN)

4.1. General

A total of 3428 data points obtained from the generated parametric study and 13 test results compiled from different resources in the literature [7-10] are used to train and validate the ANN model. The data is shown to cover a wide range of key influential parameters including various geometries, material properties with different eccentricities. The current paper aims to propose a new design formula allowing for prediction of the buckling resistance for hot-finished CHS beam-columns made from normal and high strength steel using the recent advancement of ANN. Detailed descriptions of the development of the ANN model is given in the following sections.

4.2. Neural network architecture

ANN model consists of input layer, hidden layers, and output layer. The hidden layer, consists of a set of neurons, receives weighted inputs as well as a constant bias value from each of the input nodes. The hidden layer thereafter is connected to the output layer. Each connection between the neuron in the hidden layer and output node is weighted with a value and a bias and the activation function is used to calculate the output predictions. The ANN predictions are then compared against the corresponding target values. The error between the predicted and target outputs is calculated to assess the performance of the ANN. The errors should be minimized by adjusting the weights and bias values of the ANN. This can be achieved by transferring the information (errors) from output layer toward input layer of the ANN [51]. This process is called Back-Propagation of Multilayer Feed Forward ANN. The network architecture used in this paper is a Multi-Layer Perceptron Network (MLPN) as it has been shown to be an efficient tool to model various structural members [i.e. 41, 52]. The neural network toolbox with MATLAB [53] solves a data fitting problem with a two-layer feed forward neural network and is used in this paper.

A number of key influential parameters should be identified in the ANN model including inputs, number of hidden layers, number of neurons in each hidden layer, the parameters in the output layer, and the activation function. The optimal number of the neurons in the hidden layer was defined by modelling several networks with different number of the neurons and compared together. In this paper, the ANN network was modeled with 3, 5, 7, and 9 neurons in the hidden layer, as shown in Table 5. Based on the results presented in the table, the model with 7 neurons offers a high level of accuracy and rational computational cost for the ANN model. The input parameters considered in this paper are diameter-to-thickness ratio (D/t), wall thickness (t), effective length of the columns (L_{cr}), eccentricity (e) and the yield strength of the steel (f_y). The output parameter of the ANN model is the buckling resistance of the CHS beam-column (N_u). Fig. 4 illustrates an example of ANN structure consisting of 5 input parameters, 3 neurons in the hidden layer, and 1 output parameter.

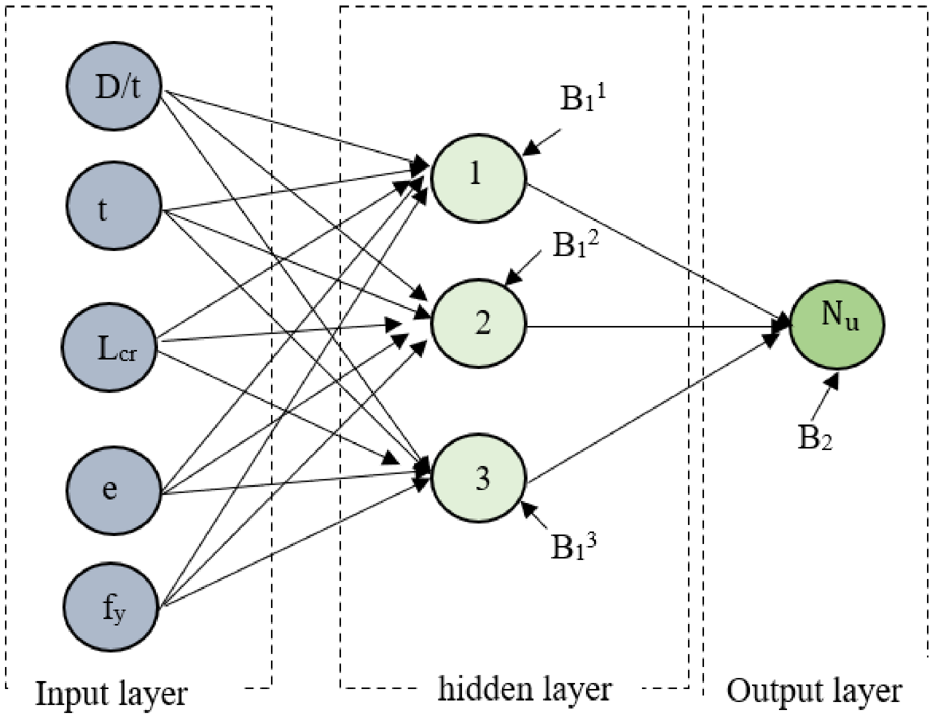

Fig. 4: (a) ANN Model with 3 neurons in the hidden layer.

4.3. Input and output normalization

The progress of training can be reduced if training data defines a region that is relatively narrow in some dimensions and elongated in others [54]. Therefore, to improve the learning speed, performance, accuracy, and stability of the training process, normalization for the input and target data should be implemented. The data can be normalized using Eq. 9 [55].

$$X^{norm} = \frac{(Y_{max} - Y_{min})(X^{act} - X_{min})}{(X_{max} - X_{min})} + Y_{min} \tag{9}$$

Table 4 illustrates the minimum and maximum values of the input/output parameters X_{min} and X_{max}, respectively. Y_{min} is the minimum value for each row of X (default is –1), Y_{max} is the maximum value for each row of X (default is +1). Y^{act} is the actual value of the input/output, and X^{norm} is the normalized value of the input/output parameter.

Table 4: Parameters used to normalize input and target values

Input/Target Parameter	X_{min}	X_{max}	Y_{min}	Y_{max}
D/t	6.667	72.482	-1	1

t (mm)	1.38	15	-1	1
L_{cr} (mm)	309.9	5249.2	-1	1
e (mm)	0	354.5	-1	1
f_y (mm)	355	900	-1	1
N_u (kN)	14.86	3274.96	-1	1

4.4. Learning (training) algorithm and transfer function

In this study, the Levenberg-Marquardt back propagation training algorithm was adopted as this algorithm is fast and has stable convergence and is suitable for training small- and medium-sized problems. In order to avoid overfitting in the ANN model, the data points are randomly divided into three sets: training, validation and testing set, with 70%, 15% and 15% of the data, respectively. During training, the 70% of the data is used to compute the gradient and update the weights and biases of the system, while cross validation occurs using the validation set so the generalization performance of the network can be verified. Once the network parameters are defined, the testing data set will be used to evaluate the accuracy of the ANN model.

This study was performed using the hyperbolic tangent transfer function which is required to determine the relationship between the output and inputs [56], as given in the Eqs. 10 and 11.

$$O_s = B_1^s + \sum_{k=1}^{r}\left(w_{k,l}^{ho}\,\frac{2}{1+\ e^{-2H_k}} - 1\right) \tag{10}$$

$$H_k =\ B_2^k + \sum_{j=1}^{q} w_{j,k}^{ih}.\,I_j \tag{11}$$

where, O_s represents the normalized output value, q is the number of input parameters; r is the number of hidden neurons; s is the number of output parameters; B_1^s and B_2^k are the biases of s^{th} output neuron and k^{th} hidden neuron (H_k), respectively; $w_{j,k}^{ih}$ is the weights of the connection between I_j and H_k; $w_{k,l}^{oh}$ is the weights of the connection between H_k and O_s.

4.5. Assessing the accuracy of neural network

To assess the accuracy and reliability of the ANN model to predict the buckling resistance of the CHS beam-column, the Regression values (R2), Root Mean Square Error (RMSE) and Mean Absolute Error (MAE) are calculated using Eqs. 12, 13 and 14 respectively.

$$R=\frac{\sum_{i=1}^{N}(O_i-\bar{O}_i)(t_i-\bar{t}_i)}{\sqrt{\sum_{i=1}^{N}(O_i-\bar{O}_i)^2\sum_{i=1}^{N}(t_i-\bar{t}_i)^2}} \tag{12}$$

$$RMSE=\sqrt{\frac{\sum_{i=1}^{N}(O_i-t_i)^2}{N}} \tag{13}$$

$$MAE=\frac{1}{N}\sum_{i=1}^{N}|O_i-t_i| \tag{14}$$

Where t_i and O_i are the actual and predicted buckling capacities, N is the total number of data points in each set of data. $\bar{O}_i$ and $\bar{t}_i$ are the average of the predicted and actual buckling resistance.

4.6. Quantifying input variable contributions in ANN using Garson's algorithm

Garson's algorithm [57] was performed to determine the relative importance of each input variable in the network, such as diameter-to-thickness, wall thickness, effective length, eccentricity and yield stress, on the buckling resistance of the CHS beam-column. In Garson's algorithm, the variable contributions are calculated based on the absolute values of the connection weights, and thus it does not provide the direction of the relationship between the input and output variables [58]. The relative importance of the j^{th} input parameter on the output is:

$$I_j=\frac{\sum_{m=1}^{m=Nh}\left(\frac{w_{jm}^{ih}}{\sum_{k=1}^{Ni}w_{km}^{ih}}w_{mn}^{ho}\right)}{\sum_{k=1}^{k=Ni}\left(\sum_{m=1}^{m=Nh}\left(\frac{w_{km}^{ih}}{\sum_{k=1}^{Ni}w_{km}^{ih}}w_{mn}^{ho}\right)\right)} \tag{15}$$

In the Eq. 15, Ni and Nh are the numbers of neurons in the input and hidden layers, respectively; w is connection weights; the superscripts i, h, and o refer to input, hidden, and output layers, respectively; and the subscripts k, m, and n refer to input, hidden, and output neurons, respectively.

5. Results

This section presents a detailed discussion and analysis of the results in terms of the optimization and validation of the ANN model, proposing the ANN-based equation for predicting the buckling resistance of the CHS beam-columns and the influence of each individual input parameter on the output variable. The performance of the proposed ANN model is assessed through a comparison with results obtained from the numerical model and those predicted using the design rules given in Eurocode 3.

5.1. Optimization and validation

Table 5 presents the statistical performance results for various ANN models obtained using different number of neurons in terms of the training, testing and validation data as well as all data set (representing the predicted outputs with respect to the corresponding actual values). The results are evaluated using statistical parameters including regression (R^2), Root Mean Squared Error (RMSE) and Mean Absolute Error (MAE). The results indicate that the accuracy of the model is improved by increasing number of neurons in hidden layers. For instance, the model with 9 neurons has R^2, RMSE and MAE values for all data set of 0.9997, 0.004 and 0.003, whereas these values for the model with 3 neurons are 0.9902, 0.023 and 0.01, respectively. It is worth noting that when the level of accuracy is barley improved with the increase in the number of neurons, there is no need to select the model with higher neurons since it may lead to overtraining issues and result in complex formulas, making design impractical. Consequently, the model with 7 neurons is selected to conduct this study since it exhibits high level of accuracy and a stable level of convergence. Furthermore, it demonstrates excellent correlation and data fitting for training, validation and testing data with regression values of 0.9975, 0.9938 and 0.9976 and RMSE values of 0.04, 0.06 and 0.18, respectively.

The accuracy of the ANN model has been further validated by comparing the ultimate buckling resistance capacities obtained from the ANN model with those obtained using FE model and experimental tests, as shown in Fig 5 and detailed in Table 5. The figure illustrates an excellent level of correlation between the predictions of the ANN model (denotes as $N_{u,ANN}$) and the corresponding actual values (which includes FE and experimental test values and denotes as $N_{u,actual}$) with R^2, RMSE and MAE values being 0.9992, 0.007 and 0.004, respectively. On the basis of the robust validation presented in this section, the ANN model has been shown to be an efficient and reliable design tools for predicting the buckling resistance capacity of hot-finished CHS beam-columns made from normal and high strength steels.

Table 5: Assessment of the ANN models with different neurons.

Number of neurons	Training		Validation		Testing		All data		
	R^2	RMSE	R^2	RMSE	R^2	RMSE	R^2	RMSE	MAE

3	0.9937	0.025	0.9978	0.013	0.9982	0.017	0.9902	0.023	0.010
5	0.9990	0.010	0.9988	0.011	0.9987	0.013	0.9979	0.011	0.006
7	0.9996	0.006	0.9992	0.008	0.9997	0.006	0.9992	0.007	0.004
9	0.9998	0.004	0.9998	0.005	0.9998	0.004	0.9997	0.004	0.003

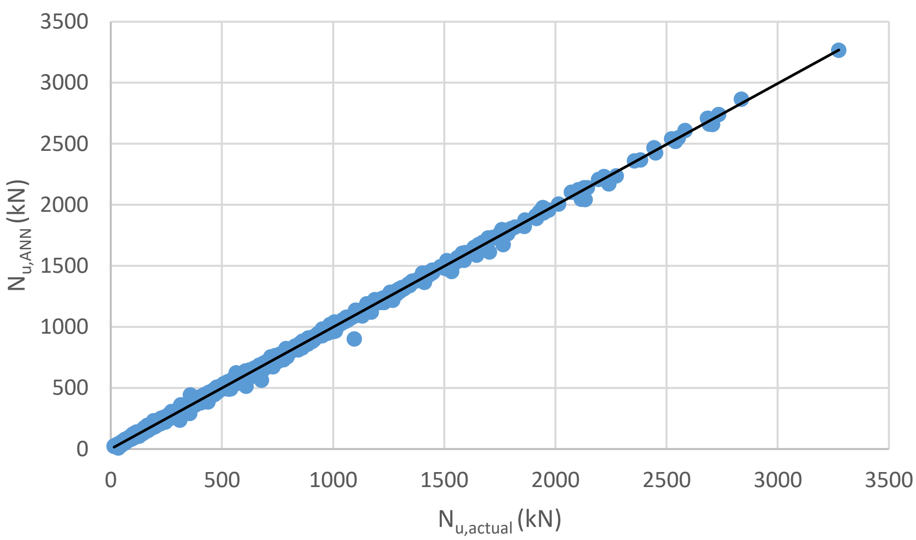

Fig. 5: Comparison between the buckling resistance capacity obtained from the ANN model (with seven neurons) and those observed numerically and experimentally.

5.2. ANN-based formula

The proposed ANN-based formula for predicting the buckling resistance of hot-finished CHS beam-columns is presented in Eq. 16. It is worth noting that the ANN-based formula is developed on the basis of normalized input values obtained using Eq. 9. Hence, denormalization process on the outputs must be applied thereafter in order to calculate the actual buckling resistance resistance of the CHS beam-columns.

$$(N_{ANN})_n = B_2 + \sum_{i=1}^{n=7} w_2(i)\left(\frac{2}{1+e^{-2H_i}} - 1\right) \tag{16}$$

$$H_i = B_1(i) + w_1(i,1)(D/t)_n + w_1(i,2)(t)_n + w_1(i,3)(L_{cr})_n + w_1(i,4)(e)_n + w_1(i,5)(f_y)_n$$

In these expressions, the parameters $(D/t)_n$, $(t)_n$, $(L_{cr})_n$, $(e)_n$, and $(f_y)_n$ represent the normalized values of the inputs D/t, t, L_{cr}, e and f_y, respectively; w1(i,j) is the connection weights between the neuron in the hidden layer (i) and input (j), whereas w2(i) is the connection weights between the neuron in the hidden layer (i) and the output. Each neuron in the hidden layer (i) has a bias value denoted as B1(i), the output bias value (B2) is equal to -1061.691. The values of w1(i,j), w2(i), and $B_1(i)$ corresponding to each neuron i are given in Table 6.

Table 6: The connection weight and the bias values.

Neuron	$w_1(i,j)$					$w_2(i)$	$B_1(i)$
	D/t	t	L_{cr}	e	f_y	N_u	
1	-0.3686	0.5797	0.7638	2.2168	-0.2174	6.2846	4.1259
2	0.4902	-0.1445	0.6595	3.5415	-0.2327	488.7007	6.1284
3	0.5032	-0.1330	0.7060	3.5471	-0.2080	-1316.0831	6.3879
4	1.2450	-0.1568	-0.0528	-0.0621	0.0416	35.5164	0.6119
5	-1.2434	0.1701	0.0527	0.0619	-0.0414	35.2565	-0.5956
6	0.3971	0.2135	-0.7443	-2.1707	0.2227	8.0896	-3.4195
7	-0.5192	0.1192	-0.7667	-3.4684	0.1771	-1889.6202	-6.9501

5.3. Importance of the input parameters

A further validation of the ANN model has been established, by analysing the contribution of the five input parameters D/t, t, L_{cr} , e and f_y on the output. The percentage contribution of each inputs to the buckling resistance of the CHS beam-columns is determined using Garson algorithm discussed in subsection 4.6 , as illustrated in Fig. 6. The contribution of each input parameter of D/t, t, L_{cr}, e and f_y are 29.8%, 6.9%, 12.4%, 46.8%, and 4.1%, respectively. Clearly, the eccentricity and the outer diameter to thickness ratio have the most significant influence on the buckling resistance capacity, while the wall thickness and steel yield stress have shown the least impact. The bearing capacity is increased with a lower values of the eccentricity and D/t ratio. This is consistent with the observations from the parametric study, as shown in Fig. 7.These results provide additional form of validation and emphasize the accuracy and reliability of the developed ANN model.

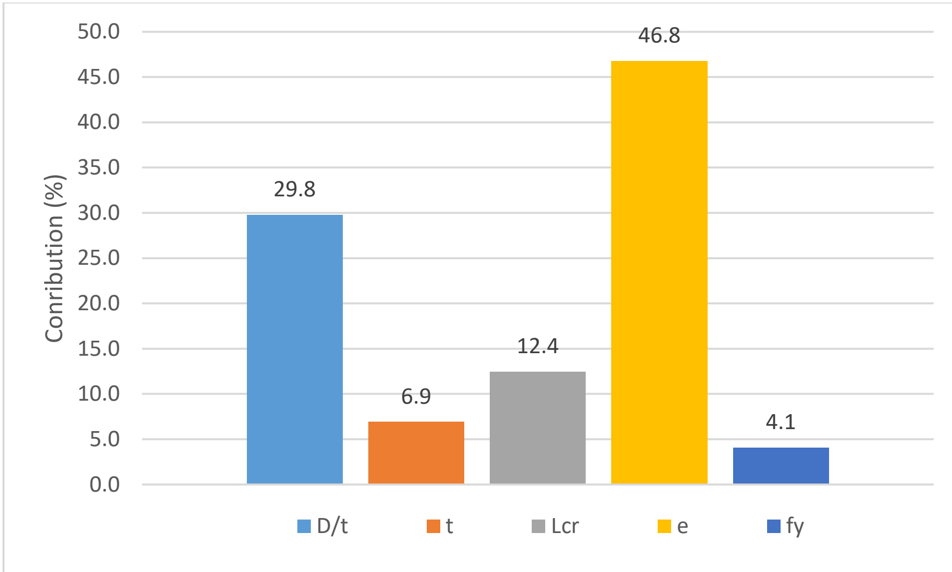

Fig. 6: Importance of the input parameters.

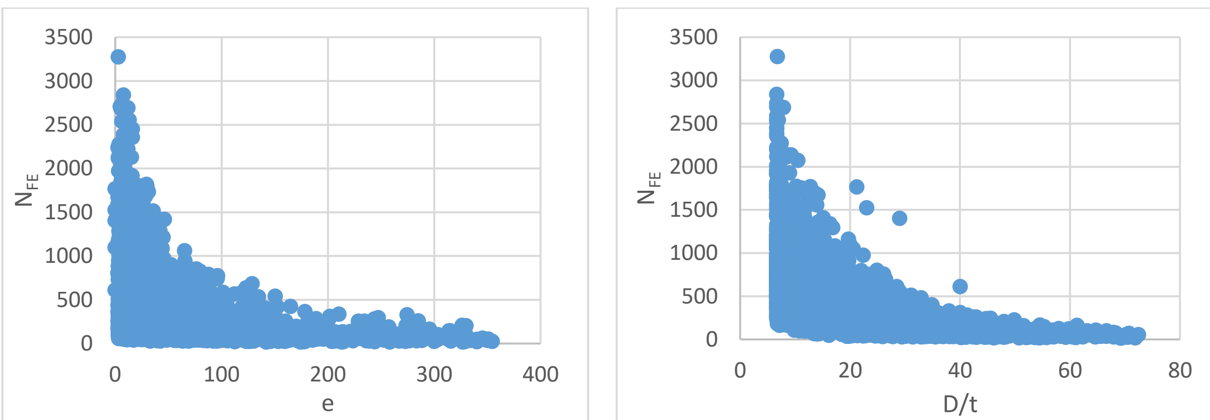

a) b)

Fig. 7: The influence of the a) eccentricity and b) the D/t ratio on the bearing capacity of the CHS beam-columns obtained from the FE model.

5.4. Comparison with design standards

The aim of this section is to assess the accuracy of proposed ANN model in the light of the current design rules given in EC3 [4] for CHS beam-columns with class 1-3 cross-sections, which are discussed previously in Section 2. The generated FE results and experimental tests collected from the literature are utilized togather with the predictions of the ANN model. Fig. 8 presents a comparison of the buckling resistance capacity obtained using the ANN model and those predicted using the design rules in EC3 in respect to the corresponding values from the FE and test results. The results presented in the figure show an excellent aggreament between the ANN resistance predictions and the corresponding actual values with the mean and coeffecient of variation (COV) values being 1 and 4.9%, repectively. On the other hand, the EC3 predections are found to be slightly conservative and less accurate compared with the ANN predictions with the mean and COV values being 0.973 and 6.3%, repectively. Furthermore, it is observed that the RMSE and MAE for the ANN model is 2.7 times lower than those of the EC3. More key statistical measures are given in Table 7 for a wider and comprehensive comparison. Obviously, the proposed ANN model is shown to be more accurat and effeicient tool to predict the buckling resistance of the CHS beam-columns with a straightforward solution and least computational cost.

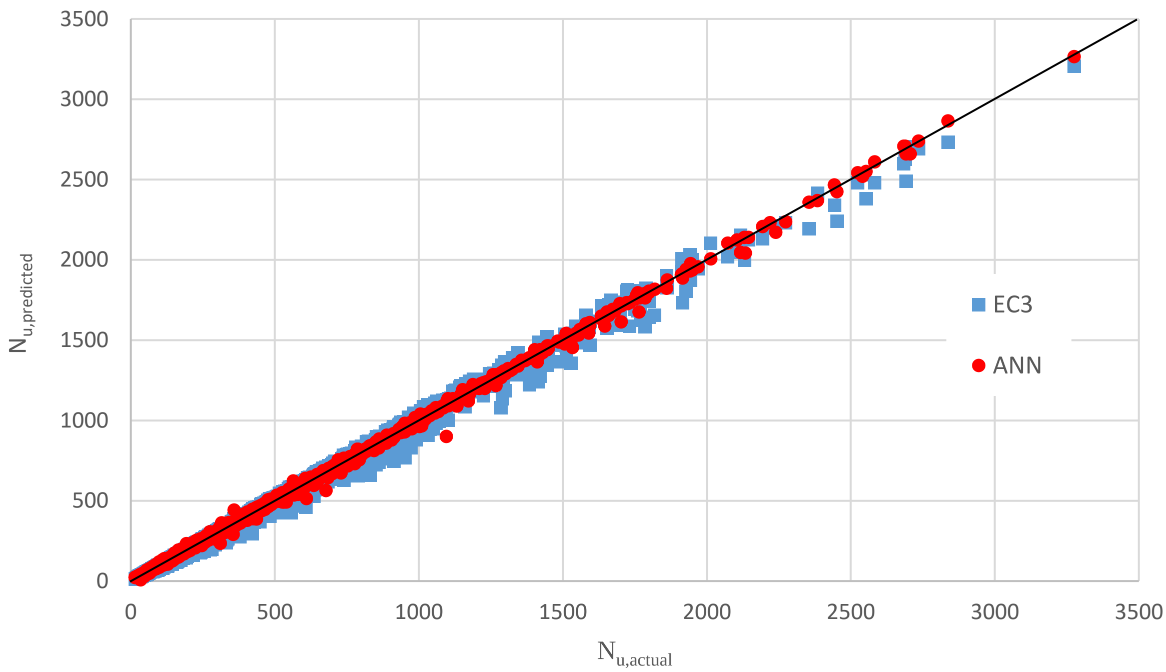

Fig. 8: Comparison of the buckling resistance of the CHS beam-columns obtained from the ANN model and EC3.

Table 7: Summary of the key statistical parameters.

	Mean	Standard deviation (%)	Coeff. of variation (%)	R^2	RMSE	MAE
$N_{u,ANN}/N_{u,actual}$	1.003	4.92%	4.91%	0.9992	9.87	6.10
$N_{u,EC3}/N_{u,actual}$	0.973	6.43%	6.61%	0.9947	28.08	15.82

Conclusions

This study has presented a detailed study into the behaviour of hot-finished CHS beam-columns made from normal and high strength steel. A particular attention is given to accurately predict the ultimate buckling resistance capacity of CHS beam-columns using the recent advancement of the artificial neural network (ANN). A total of 3439 data points were obtained from an extensive parametric study and test results available in the literature. The data is shown to cover a wide spectrum of the key parameters including various geometries, material properties with different eccentricities. The generated data is employed to train and validate the ANN model. Accordingly, a new design formula is proposed using the ANN model to predict the buckling resistance capacity of CHS beam-columns. The performance of the ANN model is further assessed through a comparison with the results obtained using the design rules given in EC3. Based on the results presented in this study, the EC3 predections are found to be slightly conservative and less accurate compared with those derived using the ANN-based design formula. However, additional experimental verifications are still required. The resulted presented in this paper emphasize the validity and accuracy of the proposed ANN-based design formula, providing an excellent basis for designers to predict the buckling resistance of the CHS beam-columns in an efficient and sustainable manner with least computational costs.

Acknowledgements

The authors are thankful to Professor Leroy Gardner and Dr Xin Meng for the collaboration in sharing the results of the FE model.

References

1. EN 1993-1-12, 2007. Eurocode 3 — Design of Steel Structures — Part 1–12: Additional Rules for the Extension of EN 1993 up to Steel Grades S 700, European Committee for Standardization (CEN), Brussels.
2. Sperle, J., Hallberg, L., Larsson, J., Groth, H., Östman, K. and Larsson, J., 2013. The environmental value of high strength steel structures. Environmental Research Programme for the Swedish Steel Industry, The Steel Eco-Cycle, pp.151-171.
3. Baddoo, N. and Chen, A., 2020. High Strength Steel Design and Execution Guide. SCI (the Steel Construction Institute).
4. prEN 1993-1-1:2020, Eurocode 3 - Design of steel structures - Part 1-1: General rules and rules for buildings, Final document, European Committee for Standardization (CEN), Brussels, 2020.

5. EN 10219-2:2019, Cold-Formed Welded Structural Hollow Sections of Non-alloy and Fine Grain Steels — Part 2: Tolerances, Dimensions and Sectional Properties, European Committee for Standardization (CEN), Brussels (2006)
6. EN 10210-2:2019, Hot-Finished Structural Hollow Sections of Non-alloy and Fine Grain Steels — Part 2: Tolerances, Dimensions and Sectional Properties European Committee for Standardization (CEN), Brussels (2006) 2006
7. Linzell, D.G., Zureick, A. and Leon, R.T., 2003. Comparison of measured and predicted response of manufactured circular steel tubular members under concentric and eccentric compressive and tensile loads. Engineering structures, 25(8), pp.1019-1031.
8. Nseir, J., 2015. Development of a new design method for the cross-section capacity of steel hollow sections (Doctoral dissertation, Université de Liège, Liège, Belgique).
9. Pournara, A.E., Karamanos, S.A., Mecozzi, E. and Lucci, A., 2017. Structural resistance of high-strength steel CHS members. Journal of Constructional Steel Research, 128, pp.152-165.
10. Hayeck, M., Nseir, J., Saloumi, E. and Boissonnade, N., 2018. Experimental characterization of steel tubular beam-columns resistance by means of the Overall Interaction Concept. Thin-Walled Structures, 128, pp.92-107.
11. Wagner, A.L., 1976. A numerical solution for the ultimate strength of tubular beam-columns.
12. Ma, J.L., Chan, T.M. and Young, B., 2017. Design of cold-formed high strength steel tubular beams. Engineering Structures, 151, pp.432-443.
13. Meng, X. and Gardner, L., 2020. Cross-sectional behaviour of cold-formed high strength steel circular hollow sections. Thin-Walled Structures, 156, p.106822.
14. Prion, H.G.L. and Birkemoe, P.C., 1992. Beam-column behavior of fabricated steel tubular members. Journal of Structural Engineering, 118(5), pp.1213-1232.
15. O'Shea, M.D. and Bridge, R.Q., 1997. Local buckling of thin-walled circular steel sections with or without internal restraint. Journal of Constructional Steel Research, 41(2-3), pp.137-157.
16. Rabi, M., Cashell, K.A., Shamass, R. and Desnerck, P., 2020. Bond behaviour of austenitic stainless steel reinforced concrete. Engineering Structures, 221, p.111027.
17. Rabi, M., Shamass, R. and Cashell, K.A., 2022. Experimental investigation on the flexural behaviour of stainless steel reinforced concrete beams. Structure and Infrastructure Engineering, pp.1-13.

18. Rabi, M., Cashell, K.A. and Shamass, R.J.E.S., 2019. Flexural analysis and design of stainless steel reinforced concrete beams. Engineering Structures, 198, p.109432.
19. Rabi, M., Shamass, R. and Cashell, K.A., 2022. Structural performance of stainless steel reinforced concrete members: A review. Construction and Building Materials, 325, p.126673.
20. Rabi, M., Cashell, K.A. and Shamass, R., 2021. Ultimate behaviour and serviceability analysis of stainless steel reinforced concrete beams. Engineering Structures, 248, p.113259.
21. Rabi, M., Cashell, K.A. and Shamass, R., 2019, May. Analysis of concrete beams reinforced with stainless steel. In Proceedings of the fib Symposium 2019: Concrete-Innovations in Materials, Design and Structures (pp. 690-697).
22. Meng, X. and Gardner, L., 2022. Stability and design of normal and high strength steel CHS beam-columns. Engineering Structures, 251, p.113361.
23. Özcan, F., Atiş, C.D., Karahan, O., Uncuoğlu, E. and Tanyildizi, H., 2009. Comparison of artificial neural network and fuzzy logic models for prediction of long-term compressive strength of silica fume concrete. Advances in Engineering Software, 40(9), pp.856-863.
24. Golafshani, E.M., Rahai, A., Sebt, M.H. and Akbarpour, H., 2012. Prediction of bond strength of spliced steel bars in concrete using artificial neural network and fuzzy logic. Construction and building materials, 36, pp.411-418.
25. Tran, V.L., Thai, D.K. and Nguyen, D.D., 2020. Practical artificial neural network tool for predicting the axial compression capacity of circular concrete-filled steel tube columns with ultra-high-strength concrete. Thin-Walled Structures, 151, p.106720.
26. Ahmadi, M., Naderpour, H. and Kheyroddin, A., 2014. Utilization of artificial neural networks to prediction of the capacity of CCFT short columns subject to short term axial load. Archives of civil and mechanical engineering, 14(3), pp.510-517.
27. Moradi, M.J., Daneshvar, K., Ghazi-Nader, D. and Hajiloo, H., 2021. The prediction of fire performance of concrete-filled steel tubes (CFST) using artificial neural network. Thin-Walled Structures, 161, p.107499.
28. Kamane, S.K., Patil, N.K. and Patagundi, B.R., 2021. Use of artificial neural network to predict the bending behavior of steel I beam externally attached with FRP sheets. Materials Today: Proceedings, 39, pp.17-21.
29. D'Aniello, M., Güneyisi, E.M., Landolfo, R. and Mermerdaş, K., 2014. Analytical prediction of available rotation capacity of cold-formed rectangular and square hollow section beams. Thin-Walled Structures, 77, pp.141-152.

30. Güneyisi, E.M., D'Aniello, M., Landolfo, R. and Mermerdaş, K., 2014. Prediction of the flexural overstrength factor for steel beams using artificial neural network. Steel and Composite Structures, 17(3), pp.215-236.
31. D'Aniello, M., Güneyisi, E.M., Landolfo, R. and Mermerdaş, K., 2015. Predictive models of the flexural overstrength factor for steel thin-walled circular hollow section beams. Thin-Walled Structures, 94, pp.67-78.
32. Hedayat, A.A., Jazebi, E., AsadAbadi, S. and Iranpour, A., 2018. Flexural strength prediction of welded flange plate connections based on slenderness ratios of beam elements using ANN. Advances in Civil Engineering, 2018.
33. Kim, J., Ghaboussi, J. and Elnashai, A.S., 2010. Mechanical and informational modeling of steel beam-to-column connections. Engineering Structures, 32(2), pp.449-458.
34. Kueh, A.B.H., 2021. Artificial neural network and regressed beam-column connection explicit mathematical moment-rotation expressions. Journal of Building Engineering, 43, p.103195.
35. Hedayat, A.A., Afzadi, E.A., Kalantaripour, H., Morshedi, E. and Iranpour, A., 2019. A new predictive model for the minimum strength requirement of steel moment frames using artificial neural network. Soil Dynamics and Earthquake Engineering, 116, pp.69-81.
36. Tohidi, S. and Sharifi, Y., 2016. Load-carrying capacity of locally corroded steel plate girder ends using artificial neural network. Thin-Walled Structures, 100, pp.48-61.
37. Sharifi, Y., Tohidi, S. and Paik, J.K., 2016. Ultimate compressive strength of deteriorated steel web plate with pitting and uniform corrosion wastage. Scientia Iranica, 23(2), pp.486-499.
38. Pu, Y. and Mesbahi, E., 2006. Application of artificial neural networks to evaluation of ultimate strength of steel panels. Engineering Structures, 28(8), pp.1190-1196.
39. Hosseinpour, M., Sharifi, Y. and Sharifi, H., 2020, October. Neural network application for distortional buckling capacity assessment of castellated steel beams. In Structures (Vol. 27, pp. 1174-1183). Elsevier.
40. Limbachiya, V. and Shamass, R., 2021. Application of artificial neural networks for web-post shear resistance of cellular steel beams. Thin-Walled Structures, 161, p.107414.
41. Ferreira, F.P.V., Shamass, R., Limbachiya, V., Tsavdaridis, K.D. and Martins, C.H., 2022. Lateral–torsional buckling resistance prediction model for steel cellular beams generated by Artificial Neural Networks (ANN). Thin-Walled Structures, 170, p.108592.

42. Tohidi, S. and Sharifi, Y., 2015. Inelastic lateral-torsional buckling capacity of corroded web opening steel beams using artificial neural networks. The IES Journal Part A: Civil & Structural Engineering, 8(1), pp.24-40.
43. Nguyen, Q.H., Ly, H.B., Le, T.T., Nguyen, T.A., Phan, V.H., Tran, V.Q. and Pham, B.T., 2020. Parametric investigation of particle swarm optimization to improve the performance of the adaptive neuro-fuzzy inference system in determining the buckling capacity of circular opening steel beams. Materials, 13(10), p.2210.
44. Gholizadeh, S., Pirmoz, A. and Attarnejad, R., 2011. Assessment of load carrying capacity of castellated steel beams by neural networks. Journal of Constructional Steel Research, 67(5), pp.770-779.
45. Rabi, M., 2023. Prediction of the bond strength capacity of stainless steel reinforcement using Artificial Neural Networks. Proceedings of the Institution of Civil Engineers-Construction Materials, pp.1-25.
46. Rabi, M., Ferreira, F., Abarkan, I., Limbachiya, V. and Shamass, R., 2023. Prediction of the cross-sectional capacity of cold-formed CHS using numerical modelling and machine learning. Results in Engineering, p.100902.
47. Dassault Systèmes. (2016) Abaqus user's Guide Manual [Computer program]. http://dixon:2080/texis/search/?query=concrete+materialandgroup=bkandCDB=v2016andsubmit.x=0andsubmit.y=0.
48. Meng, X., Gardner, L., Sadowski, A.J., Rotter, J.M., 2020. Elasto-plastic behaviour and design of semi compact circular hollow sections. Thin-Walled Structures, 148, p.106486.
49. Buchanan, C., Real, E. and Gardner, L., 2018. Testing, simulation and design of cold-formed stainless steel CHS columns. Thin-Walled Structures, 130, pp.297-312.
50. Wang, J., Afshan, S., Gkantou, M., Theofanous, M., Baniotopoulos, C. and Gardner, L., 2016. Flexural behaviour of hot-finished high strength steel square and rectangular hollow sections. Journal of Constructional Steel Research, 121, pp.97-109.
51. Ahmad, A., Cotsovos, D.M. and Lagaros, N.D., 2016. Assessing the reliability of RC code predictions through the use of artificial neural network. In 1st international conference on structural safety under fire & blast. Glasgow, UK.
52. Sharifi, Y., Moghbeli, A., Hosseinpour, M. and Sharifi, H., 2020. Study of neural network models for the ultimate capacities of cellular steel beams. Iranian Journal of Science and Technology, Transactions of Civil Engineering, 44(2), pp.579-589.
53. MATLAB and Statistics Toolbox Release 2019a, The MathWorks, Inc., Natick, Massachusetts, United States.

54. Abambres, M., Rajana, K., Tsavdaridis, K.M. and Ribeiro, T.P. (2018). Neural network-based formula for the buckling load prediction of I-section cellular steel beams. Computers, 8(1), pp.1-26.
55. Jin, J., Li, M. and Jin, L., 2015. Data normalization to accelerate training for linear neural net to predict tropical cyclone tracks. Mathematical Problems in Engineering, 2015.
56. Moradi, M.J., Khaleghi, M., Salimi, J., Farhangi, V. and Ramezanianpour, A.M., 2021. Predicting the compressive strength of concrete containing metakaolin with different properties using ANN. Measurement, 183, p.109790.
57. Garson, D.G., 1991. Interpreting neural network connection weights.
58. Olden, J.D. and Jackson, D.A., 2002. Illuminating the “black box”: a randomization approach for understanding variable contributions in artificial neural networks. Ecological modelling, 154(1-2), pp.135-150.